

10. DATA REPORT: MULTIPROXY GEOCHEMICAL CHARACTERIZATION OF OAE-RELATED BLACK SHALES AT SITE 1276, NEWFOUNDLAND BASIN¹

Michela Arnaboldi² and Philip A. Meyers²

ABSTRACT

During Ocean Drilling Program Leg 210, a greatly expanded sedimentary sequence of continuous Cretaceous black shales was recovered at Site 1276. This section corresponds to the Hatteras Formation, which has been documented widely in the North Atlantic Ocean. The cored sequence extends from the lowermost Albian, or possibly uppermost Aptian, to the Cenomanian/Turonian boundary and is characterized by numerous gravity-flow deposits and sporadic, finely laminated black shales. The sequence also includes several sedimentary intervals with high total organic carbon (TOC) contents, in several instances of probable marine origin that may record oceanic anoxic events (OAE). These layers might correspond to the Cenomanian–Turonian OAE 2; the mid-Cenomanian event; and OAE 1b, 1c, and 1d in the Albian. In addition, another interval with geochemical characteristics similar to OAE-type layers was recognized in the Albian, although it does not correspond to any of the known OAEs. This study investigates the origin of the organic matter contained within these black shale intervals using TOC and CaCO₃ contents, C_{org}/N_{tot} ratios, organic carbon and nitrogen isotopes, trace metal composition, and rock-eval analyses. Most of these black shale intervals, especially OAE 2 and 1b, are characterized by low δ¹⁵N values (<0‰) commonly observed in mid-Cretaceous black shales, which seem to reflect the presence of an altered nitrogen cycle with rates of nitrogen fixation significantly higher than in the modern ocean.

¹Arnaboldi, M., and Meyers, P.A., 2006. Data report: multiproxy geochemical characterization of OAE-related black shales at Site 1276, Newfoundland Basin. In Tucholke, B.E., Sibuet, J.-C., and Klaus, A. (Eds.), *Proc. ODP, Sci. Results*, 210: College Station, TX (Ocean Drilling Program), 1–16.

doi:10.2973/odp.proc.sr.210.102.2006

²Marine Geology and Geochemistry Program, Department of Geological Sciences, The University of Michigan, 1100 North University Avenue, Ann Arbor MI 48109-1063, USA.

Correspondence author:
marna@umich.edu

INTRODUCTION

A greatly expanded sedimentary sequence of virtually continuous Cretaceous black shales characterized by moderately enriched total organic carbon (TOC) contents (mostly ≤ 2 wt%) was cored at Ocean Drilling Program Leg 210 Site 1276. The sequence extends from the lowermost Albian, or possibly uppermost Aptian, to the Cenomanian/Turonian boundary and is considered to be equivalent to the Hatteras Formation (Jansa et al., 1979). Based on preliminary geochemical analyses and palynological data, much of the organic matter preserved in these hemipelagic and turbiditic sediments is likely of terrigenous origin and was deposited under dysoxic/anoxic conditions (Shipboard Scientific Party, 2004).

The mid-Cretaceous (~124–90 Ma) was characterized by warm global climate and rising sea level (e.g., Wilson and Norris, 2001). Periodically, organic carbon-rich black shales were deposited in response to the development of dysoxic and anoxic conditions in oxygen-minimum zones along the continental margins of the tropical Tethys Sea, in restricted epicontinental seas, and in basins of the widening North and South Atlantic.

The Cretaceous sequence recovered during Leg 210 includes six sedimentary intervals with high TOC contents, in several instances of probable marine origin, which may record oceanic anoxic events (OAEs). These include the Cenomanian–Turonian OAE 2 (“Bonarelli” event); the “mid-Cenomanian” event; and OAE 1b (“Paquier” event), 1c, and 1d in the Albian (Leckie et al., 2002, and references therein). In addition, another interval with OAE-like geochemical characteristics and located between OAEs 1c and 1b was recognized in the Albian, although it does not correspond to any of the known OAEs.

The recovery of sediments geochemically comparable to OAE-related black shales in the Newfoundland Basin is especially important in that it allows the investigation of paleoceanographic links between this part of the expanding Cretaceous North Atlantic and the rest of the world ocean. Here we report the results of shorebased analyses of the carbon and nitrogen stable isotope compositions of organic matter, rock-eval pyrolysis of bulk organic matter, and major and trace metal compositions of whole-sediment samples.

METHODS

All samples were freeze-dried overnight and subsequently ground. Concentrations of calcium carbonate were determined using the “carbonate bomb” technique (Müller and Gastner, 1971), which measures the volume of CO₂ released by treatment of the sediments with 3-N HCl. Inorganic carbon concentrations were calculated assuming that all inorganic carbon is present as CaCO₃.

The carbonate-free residues were washed and rinsed three times with deionized water, oven dried, and analyzed for organic carbon and total nitrogen (TN) using a Carlo Erba EA1108 CHNS-O analyzer. Relative precision for carbon is $\pm 2\%$ and $\pm 3\%$ for nitrogen. TOC and TN concentrations are expressed on a whole-sediment basis after adjusting for the removed carbonate fraction. C_{org}/N_{tot} ratios are calculated on an atomic basis.

The $\delta^{15}\text{N}$ and $\delta^{13}\text{C}_{\text{org}}$ values of bulk organic matter were determined on the carbonate-free sediments using a continuous-flow gas-ratio mass spectrometer (Finnigan Delta Plus XL) coupled to an elemental analyzer (Costech) at the Laboratory of Isotope Geochemistry, University of Arizona (USA). Data are expressed in the conventional $\delta^{15}\text{N}$ and $\delta^{13}\text{C}$ notations relative to air and PeeDee belemnite standard, respectively. Standardization is based on International Atomic Energy Agency (IAEA)-N-1 and IAEA-N-2 for $\delta^{15}\text{N}$, and National Bureau of Standards-22 and U.S. Geological Survey-24 for $\delta^{13}\text{C}$. Precision is better than $\pm 0.2\text{‰}$ for $\delta^{15}\text{N}$ and $\pm 0.06\text{‰}$ for $\delta^{13}\text{C}$, based on repeated internal standards.

Freeze-dried ground sediment samples were analyzed by programmed pyrolysis at the Institute of Sedimentary and Petroleum Geology of the Geological Survey of Canada (Calgary, Alberta) using a Delsi Nermag Rock-Eval 6 system. The Rock-Eval 6 yields T_{max} values that are systematically higher than those from the Rock-Eval 2 system that is the basis for T_{max} interpretations, so the values we report have been adjusted to the Rock-Eval 2 standard.

For determination of the major and minor element compositions, samples were prepared using a sodium peroxide digest technique modified from Knoop (2005). Approximately 0.1000 g of sample was well mixed with 1 g of sodium peroxide in a zirconium crucible and heated in a 500°C oven for 30 min. After cooling to room temperature, 5 mL of 5% HNO_3 was slowly added to the solid residue in the crucible and the sample was transferred to a 60-mL Nalgene bottle. Next, 15 mL of 5% HNO_3 was added to the bottle along with 5 drops of concentrated HCl and 20 drops of HF. The total sample volume was brought to ~50 mL with additional 5% HNO_3 . Samples were shaken by hand for ~30 s, at which time no visible solid residue remained. Elemental analyses of Al, Ti, Fe, Mg, K, Ba, Cr, and Zn were carried out by inductively coupled plasma-optical emission spectrometer (ICP-OES) using a PerkinElmer Optima 3300DV. Analyses for Cd, Cu, Mo, Re, U, and V were carried out by ICP-mass spectroscopy (MS) on a Finnegan Element mass spectrometer.

RESULTS

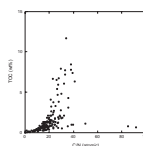
Organic Carbon Concentrations and $\text{C}_{\text{org}}/\text{N}_{\text{tot}}$ Ratios

TOC concentrations vary between 0 and 11.7 wt% in the Cretaceous sequence (Table T1). Virtually all samples with TOC > 2 wt% are from the OAE-related black shale intervals.

$\text{C}_{\text{org}}/\text{N}_{\text{tot}}$ ratios range between 1.5 and 91.7 (Table T1), with most samples having values <40 (Fig. F1). $\text{C}_{\text{org}}/\text{N}_{\text{tot}}$ ratios are often used as indicators of the origin of organic matter, with lower values (4–10) being typical of marine algae and higher values (>20) considered to be typical of land-derived material (Meyers, 1994). However, many Cretaceous black shales (Meyers et al., 1984; Meyers, 1987) and Mediterranean sapropels (Bouloubassi et al., 1999; Meyers and Doose, 1999; Nijenhuis and de Lange, 2000) have high $\text{C}_{\text{org}}/\text{N}_{\text{tot}}$ ratios even though the organic matter appears to be marine-derived. The correspondence of high $\text{C}_{\text{org}}/\text{N}_{\text{tot}}$ ratios with high TOC percentages, as observed in the samples from Site 1276 (Fig. F1), has been postulated to result from a coupling between higher fluxes of organic matter and improved preservation of its carbon content relative to its nitrogen content (Twichell et al., 2002). This diagenetic process is promoted by water-column suboxic

T1. Carbon, C/N, and isotopic values, p. 11.

F1. TOC and C/N, p. 8.



conditions and appears to be associated with denitrification (Van Mooy et al., 2002).

Organic Carbon and Total Nitrogen Isotopic Compositions

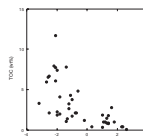
Values of $\delta^{13}\text{C}_{\text{org}}$ vary from $-28.3\text{\textperthousand}$ to $-19.6\text{\textperthousand}$ in the sequence (Table T1), although almost all samples show $\delta^{13}\text{C}_{\text{org}}$ at less than $-22\text{\textperthousand}$ (Table T1). Values of $\delta^{13}\text{C}_{\text{org}}$ are commonly used as an origin indicator of organic matter with higher values (from $-25\text{\textperthousand}$ to $-20\text{\textperthousand}$), typical of modern marine phytoplankton, and lower values typical of terrestrial plants (from $-30\text{\textperthousand}$ to $-27\text{\textperthousand}$). However, the mid-Cretaceous was a greenhouse world with high $p\text{CO}_2$. The availability of dissolved CO_2 impacts the carbon isotopic composition of algal organic matter because biological discrimination in favor of ^{12}C increases when $p\text{CO}_2$ is high and decreases when it is low (e.g., Fogel and Cifuentes, 1993). For this reason, marine organic matter produced in the Cretaceous commonly has $\delta^{13}\text{C}$ values from $-28\text{\textperthousand}$ to $-25\text{\textperthousand}$ (e.g., Rau et al., 1987), which is similar to modern C_3 land plants. Nonetheless, organic carbon isotopic compositions can still be used to reconstruct past productivity rates because during episodes of enhanced productivity algal discrimination decreases, producing higher $\delta^{13}\text{C}_{\text{org}}$ values. These higher $\delta^{13}\text{C}_{\text{org}}$ values are common in OAEs, and most of our samples within the OAE-related black shale interval present somewhat higher $\delta^{13}\text{C}_{\text{org}}$ values (greater than $-26\text{\textperthousand}$).

Values of $\delta^{15}\text{N}$ range between $-3.2\text{\textperthousand}$ and $2.6\text{\textperthousand}$, with most samples having $\delta^{15}\text{N}$ values $<0\text{\textperthousand}$ (Table T1; Fig. F2). Like carbon, nitrogen isotopes can also be used as a source and/or paleoproductivity indicator. Marine algae in the modern ocean are commonly characterized by higher $\delta^{15}\text{N}$ values (from $+7\text{\textperthousand}$ to $+10\text{\textperthousand}$), whereas land plants average $\sim 0\text{\textperthousand}$. Values of $\delta^{15}\text{N}$ can reflect variable nutrient uptake because of higher nitrogen fractionation (lower $\delta^{15}\text{N}$ values) with high nitrate availability (Calvert et al., 1992). More importantly, $\delta^{15}\text{N}$ values of sediment organic matter are also sensitive to processes that deeply affect the nitrogen cycle, such as nitrogen fixation. Low $\delta^{15}\text{N}$ values, common in mid-Cretaceous black shales, can reflect shifts in the mode of primary marine production from algae to microbes (Rau et al., 1987), in which nitrogen fixers become the dominant producers. Values of $\delta^{15}\text{N}$ are inversely related to TOC concentrations in our samples. Samples with higher TOC contents are characterized by negative nitrogen isotopes, which is especially evident for $\text{TOC} > 5 \text{ wt\%}$ (Fig. F2). These samples are within the OAE-related black shales and their low $\delta^{15}\text{N}$ values suggest that these layers were deposited during periods characterized by an altered nitrogen cycle when nitrogen fixation rates were significantly higher in the surface ocean.

Rock-Eval Results

Rock-eval analyses help to identify the type (marine, bacterial, or terrigenous) and maturity of sedimentary organic matter (e.g., Meyers, 1996). We report a suite of parameters and indexes obtained from this analysis in Table T2. Land-plant organic matter tends to be rich in woody components and consequently has lower hydrogen indexes (HIs) and higher oxygen indexes (OIs) than found in lipid-rich and cel-

F2. TOC and $\delta^{15}\text{N}$, p. 9.



T2. Rock-eval results, p. 14.

lulose-poor algal organic matter. Diagenesis, however, can cause marine organic matter to gradually acquire HI and OI values similar to those of land plant material or cause its degradation to detrital, Type IV organic matter (Meyers, 1996). The T_{\max} of all samples from Site 1276 are <435°C (Table T2), which indicates that the organic matter is thermally immature with respect to petroleum generation (Espitalié et al., 1977). Additionally, a Van Krevelen-type plot of the HI and OI values of all samples (Fig. F3) indicates that their organic matter is a mixture of continental and oxidized marine material (Meyers, 1996). In particular, the samples from the OAE 2 and OAE 1b-related black shales (low OI and high HI) seem to contain Type I or II marine-derived organic matter (Table T2).

Trace Element Compositions

Major and minor element compositions are useful to evaluate changes in paleoproductivity rates, preservation of organic matter, and paleoenvironmental conditions. A normalization of the elemental concentrations to Al is commonly used (e.g., Wehausen and Brumsack, 1999; Warning and Brumsack, 2000; Rinna et al., 2002) in order to compensate for clastic or carbonate dilution. Aluminum is not influenced by biogenic activity, authigenic enrichment, or diagenetic dissolution (Rinna et al., 2002).

Mild enrichments of redox-sensitive and chalcophile elements (U, Re, Cu, Mo, Cr, V, Cd, and Zn), such as the ones observed in our samples (Tables T3, T4), likely indicate deposition in an oxygen-poor environment (van Santvoort et al., 1997; Nijenhuis et al., 1998; Schenau et al., 1999; Hofmann et al., 2001; Arnaboldi and Meyers, 2003). These elements are precipitated from seawater and their accumulation and immobilization in sediment is associated with dysoxic/anoxic conditions either in the water column or in the sediment. Finally, Ba, which is generally a good proxy for paleoproductivity, especially in the deep ocean (e.g., Dymond et al., 1992), presents moderate enrichments in our samples (Tables T3, T4).

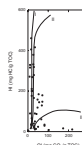
ACKNOWLEDGMENTS

We thank Andrea Klaue for her help in the sample preparation, Carmen Nezat for the ICP-OES analyses, and Ted Huston for the ICP-MS analyses. Thanks are due to Chris Eastoe at the University of Arizona for the nitrogen and carbon isotope analyses. We also thank Lloyd Snowden for the rock-eval analyses.

This research used samples and data provided by the Ocean Drilling Program (ODP). ODP is sponsored by the U.S. National Science Foundation (NSF) and participating countries under management of Joint Oceanographic Institutions (JOI), Inc. A grant to P.A.M. from the U.S. Sciences Support Program helped fund this study.

We thank Adam Klaus and an anonymous reviewer for providing helpful and constructive reviews of this manuscript.

F3. HI and OI, p. 10.



T3. Trace and element oxides, p. 15.

T4. Element/Al ratios, p. 16.

REFERENCES

- Arnaboldi, M., and Meyers, P.A., 2003. Geochemical evidence for paleoclimatic variations during deposition of two late Pliocene sapropels from the Vrica section, Calabria. In Meyers, P.A., and Negrini, A. (Eds.), *Paleoclimatic and Paleoceanographic Records in Mediterranean Sapropels and Mesozoic Black Shales*. Palaeogeogr., Palaeoclimatol., Palaeoecol., 190:257–271. doi:[10.1016/S0031-0182\(02\)00609-0](https://doi.org/10.1016/S0031-0182(02)00609-0)
- Bouloubassi, I., Rullkötter, J., and Meyers, P.A., 1999. Origin and transformation of organic matter in Pliocene-Pleistocene Mediterranean sapropels: organic geochemical evidence reviewed. *Mar. Geol.*, 153(1–4):177–197. doi:[10.1016/S0025-3227\(98\)00082-6](https://doi.org/10.1016/S0025-3227(98)00082-6)
- Calvert, S.E., Nielsen, B., and Fontugne, M.R., 1992. Evidence from nitrogen isotope ratios for enhanced productivity during formation of eastern Mediterranean sapropels. *Nature (London, U.K.)*, 359:223–225. doi:[10.1038/359223a0](https://doi.org/10.1038/359223a0)
- Dymond, J., Suess, E., and Lyle, M., 1992. Barium in deep-sea sediment: a geochemical proxy for paleoproductivity. *Paleoceanography*, 7:163–181.
- Espitalié, J., Laporte, J.L., Madec, M., Marquis, F., Leplat, P., Paulet, J., and Bouteleau, A., 1977. Méthode rapide de caractérisation des roches mères, de leur potentiel pétrolier et de leur degré d'évolution. *Rev. Inst. Fr. Pet.*, 32:23–42.
- Fogel, M.L., and Cifuentes, L.A., 1993. Isotope fractionation during primary production. In Engel, M.H., and Macko, S.A. (Eds.), *Organic Geochemistry: Principles and Applications*: New York (Plenum), 73–98.
- Hofmann, P., Ricken, W., Schwark, L., and Leythaeuser, D., 2001. Geochemical signature and related climatic-oceanographic process for early Albian black shales: Site 417D, North Atlantic Ocean. *Cretaceous Res.*, 22:243–257. doi:[10.1006/cres.2001.0253](https://doi.org/10.1006/cres.2001.0253)
- Jansa, L.F., Enos, P., Tucholke, B.E., Gradstein, F.M., and Sheridan, R.E., 1979. Mesozoic-Cenozoic sedimentary formations of the North American Basin, western North Atlantic. In Talwani, M., Hay, W., and Ryan, W.B.F. (Eds.), *Deep Drilling Results in the Atlantic Ocean: Continental Margins and Paleoenvironment*. Maurice Ewing Ser., 3:1–57.
- Knoop, P.A., 2005. Data report: Inorganic geochemistry of hydrothermal sediments, Hole 1215A. In Wilson, P.A., Lyle, M., and Firth, J.V. (Eds.), *Proc. ODP, Sci. Results*, 199 [Online]. Available from World Wide Web: <http://www-odp.tamu.edu/publications/199_SR/218/218.htm>. [Cited 2005-11-21]
- Leckie, R.M., Bralower, T.J., and Cashman, R., 2002. Oceanic anoxic events and plankton evolution: biotic response to tectonic forcing during the mid-Cretaceous. *Paleoceanography*, 17(3):1041. doi:[10.1029/2001PA000623](https://doi.org/10.1029/2001PA000623)
- Meyers, P.A., 1987. Organic-carbon content of sediments and rocks from Deep Sea Drilling Project Sites 603, 604, and 605, western margin of the North Atlantic. In van Hinte, J.E., Wise, S.W., Jr., et al., *Init. Repts. DSDP*, 93 (Pt. 2): Washington (U.S. Govt. Printing Office), 1187–1194.
- Meyers, P.A., 1994. Preservation of elemental and isotopic source identification of sedimentary organic matter. *Chem. Geol.*, 114(3–4):289–302. doi:[10.1016/0009-2541\(94\)90059-0](https://doi.org/10.1016/0009-2541(94)90059-0)
- Meyers, P.A., 1996. Geochemical comparisons of organic matter in Cretaceous black shales from Site 897, Iberia Abyssal Plain, Sites 638 and 641, Galicia Margin, and Site 398, Vigo Seamount. In Whitmarsh, R.B., Sawyer, D.S., Klaus, A., and Masson, D.G. (Eds.), *Proc. ODP, Sci. Results*, 149: College Station, TX (Ocean Drilling Program), 295–300. doi:[10.2973/odp.proc.sr.149.240.1996](https://doi.org/10.2973/odp.proc.sr.149.240.1996)
- Meyers, P.A., and Doose, H., 1999. Sources, preservation, and thermal maturity of organic matter in Pliocene-Pleistocene organic-carbon-rich sediments of the western Mediterranean Sea. In Zahn, R., Comas, M.C., and Klaus, A. (Eds.), *Proc. ODP, Sci. Results*, 161: College Station, TX (Ocean Drilling Program), 383–390. doi:[10.2973/odp.proc.sr.161.235.1999](https://doi.org/10.2973/odp.proc.sr.161.235.1999)

- Meyers, P.A., Leenheer, M.J., Kawka, O.E., and Trull, T.W., 1984. Enhanced preservation of marine-derived organic matter in Cenomanian black shales from the southern Angola Basin. *Nature (London, U. K.)*, 312:356–359. [doi:10.1038/312356a0](https://doi.org/10.1038/312356a0)
- Müller, G., and Gastner, M., 1971. The “Karbonate-Bombe,” a simple device for the determination of the carbonate content in sediments, soils, and other materials. *Neues Jahrb. Mineral.*, 10:466–469.
- Nijenhuis, I.A., Brumsack, H.-J., and de Lange, G.J., 1998. The trace element budget of the Eastern Mediterranean during Pliocene sapropel formation. In Robertson, A.H.F., Emeis, K.-C., Richter, C., and Camerlenghi, A. (Eds.), *Proc. ODP, Sci. Results*, 160: College Station, TX (Ocean Drilling Program), 199–206. [doi:10.2973/odp.proc.sr.160.019.1998](https://doi.org/10.2973/odp.proc.sr.160.019.1998)
- Nijenhuis, I.A., and de Lange, G.J., 2000. Geochemical constraints on Pliocene sapropel formation in the eastern Mediterranean. *Mar. Geol.*, 163:41–63. [doi:10.1016/S0025-3227\(99\)00093-6](https://doi.org/10.1016/S0025-3227(99)00093-6)
- Rau, G.H., Arthur, M.A., and Dean, W.E., 1987. $^{15}\text{N}/^{14}\text{N}$ variations in Cretaceous Atlantic sedimentary sequences: implication for past changes in marine nitrogen biogeochemistry. *Earth Planet. Sci. Lett.*, 82(3–4):269–279. [doi:10.1016/0012-821X\(87\)90201-9](https://doi.org/10.1016/0012-821X(87)90201-9)
- Rinna, J., Warning, B., Meyers, P.A., Brumsack, H.J., and Rullkötter, J., 2002. Combined organic and inorganic geochemical reconstruction of paleodepositional conditions of a Pliocene sapropel from the eastern Mediterranean Sea. *Geochim. Cosmochim. Acta*, 66(11):1969–1986. [doi:10.1016/S0016-7037\(02\)00826-8](https://doi.org/10.1016/S0016-7037(02)00826-8)
- Schenau, S.J., Antonarakou, A., Hilgen, F.J., Lourens, L.J., Nijenhuis, I.A., van der Weijden, C.H., and Zachariasse, W.J., 1999. Organic-rich layers in the Metochia sections (Gavdos, Greece): evidence for a single mechanism of sapropel formation during the last 10 My. *Mar. Geol.*, 153(1–4):117–135. [doi:10.1016/S0025-3227\(98\)00086-3](https://doi.org/10.1016/S0025-3227(98)00086-3)
- Shipboard Scientific Party, 2004. Site 1276. In Tucholke, B.E., Sibuet, J.-C., Klaus, A., et al., *Proc. ODP, Init. Repts.*, 210: College Station, TX (Ocean Drilling Program), 1–358. [doi:10.2973/proc.odp.ir.210.103.2004](https://doi.org/10.2973/proc.odp.ir.210.103.2004)
- Twichell, S.C., Meyers, P.A., and Diester-Haass, L., 2002. Significance of high C/N ratios in organic-carbon-rich Neogene sediments under the Benguela Current upwelling system. *Org. Geochem.*, 33(7):715–722. [doi:10.1016/S0146-6380\(02\)00042-6](https://doi.org/10.1016/S0146-6380(02)00042-6)
- Van Mooy, B.A.S., Keil, R.G., and Devol, A.H., 2002. Impact of suboxia on sinking particulate organic carbon: enhanced carbon flux and preferential degradation of amino acids via denitrification. *Geochim. Cosmochim. Acta*, 66(3):457–465. [doi:10.1016/S0016-7037\(01\)00787-6](https://doi.org/10.1016/S0016-7037(01)00787-6)
- van Santvoort, P.J.M., de Lange, G.J., Langereis, C.G., Dekkers, M.J., and Paterne, M., 1997. Geochemical and paleomagnetic evidence for the occurrence of “missing” sapropels in eastern Mediterranean sediments. *Paleoceanography*, 12(6):773–786. [doi:10.1029/97PA01351](https://doi.org/10.1029/97PA01351)
- Warning, B., and Brumsack, H.-J., 2000. Trace metal signatures of eastern Mediterranean sapropels. *Palaeogeogr., Palaeoclimatol., Palaeoecol.*, 158(3–4):293–309. [doi:10.1016/S0031-0182\(00\)00055-9](https://doi.org/10.1016/S0031-0182(00)00055-9)
- Wehausen, R., and Brumsack, H.-J., 1999. Cyclic variations in the chemical composition of eastern Mediterranean Pliocene sediments: a key for understanding sapropel formation. *Mar. Geol.*, 153(1–4):161–176. [doi:10.1016/S0025-3227\(98\)00083-8](https://doi.org/10.1016/S0025-3227(98)00083-8)
- Wilson, P.A., and Norris, R.D., 2001. Warm tropical ocean surface and global anoxia during the mid-Cretaceous period. *Nature (London, U. K.)*, 412:425–429. [doi:10.1038/35086553](https://doi.org/10.1038/35086553)

Figure F1. Comparison of total organic carbon (TOC) contents and atomic $C_{\text{org}}/N_{\text{tot}}$ ratios for Site 1276 samples listed in Table T1, p. 11.

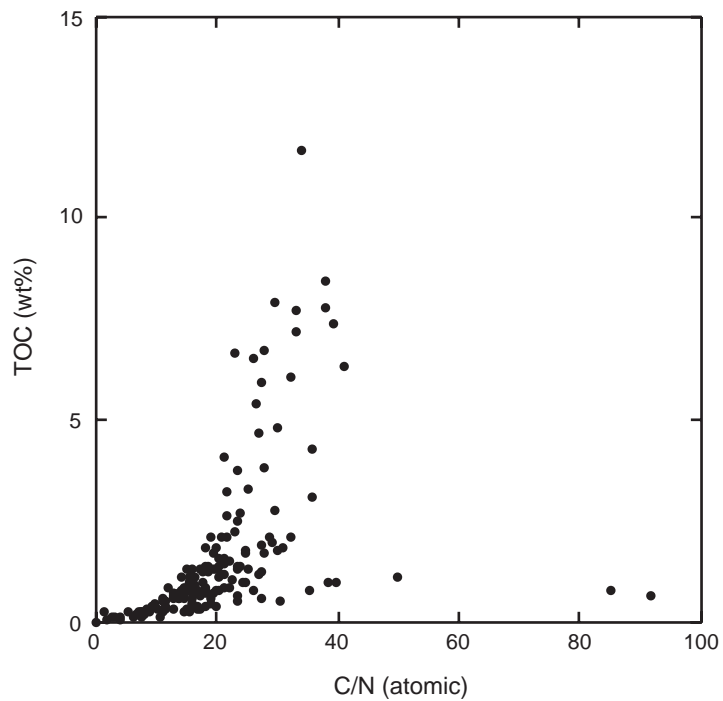


Figure F2. Comparison of total organic carbon (TOC) contents and $\delta^{15}\text{N}$ values for Site 1276 samples listed in Table T1, p. 11.

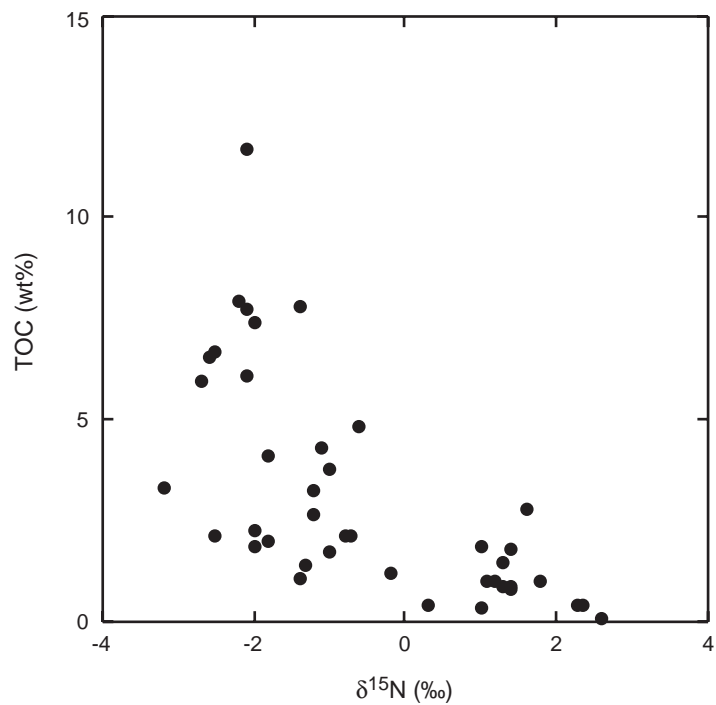


Figure F3. Comparison of hydrogen index (HI) and oxygen index (OI) for Site 1276 samples listed in Table T2, p. 14. Diagenetic pathways of kerogen Types I, II, and III are shown (modified from Meyers, 1996). HC = hydrocarbon, TOC = total organic carbon.

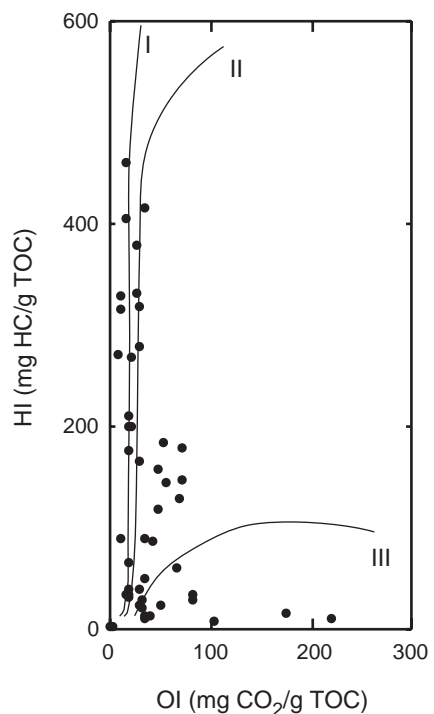


Table T1. Carbon concentrations, C/N ratios, and isotopic values of selected mid-Cretaceous samples, Site 1276. (See table notes. Continued on next two pages.)

Core, section, interval (cm)	Depth (mbsf)	Age	OAE	CaCO ₃ (wt%)	TOC (wt%)	C _{org} /N _{tot} (atomic)	¹³ C (‰)	¹⁵ N (‰)
210-1276A-								
30R-1, 0–1	1069.40			0.0	0.34	16.7		
30R-1, 18–19	1069.58			22.5	0.24	7.7		
30R-2, 11–12	1070.87			12.7	0.69	19.5		
30R-3, 0–1	1072.13			7.2	0.30	10.3		
30R-3, 12–13	1072.25	Turonian		3.2	0.40	16.9	-25.14	2.3
30R-4, 47–48	1074.10			0.0	6.65	22.9	-26.52	-2.51
30R-4, 78–79	1074.41			5.8	0.53	11.1		
30R-4, 115–116	1074.78			0.0	1.38	18.6	-25.65	-1.26
30R-4, 128–129	1074.91			0.0	0.13	2.6		
30R-5, 33–34	1075.46			11.3	1.14	20.6	-25.8	-0.15
31R-1, 0–1	1079.00			6.2	0.36	9.5	-25.36	0.3
31R-1, 65–66	1079.65			10.4	0.32	11.5		
31R-1, 111–113	1080.11			15.5	0.12	4.0		
31R-1, 140–142	1080.40			0.4	6.54	26.1	-26.01	-2.57
31R-2, 15–18	1080.65			0.0	0.09	3.1		
31R-2, 23–26	1080.73			0.0	2.67	24.0		
31R-2, 59–62	1081.09			1.7	11.67	33.9	-24.22	-2.13
31R-2, 80–83	1081.30			0.5	8.44	37.9		
31R-2, 124–128	1081.74			0.0	3.78	27.8		
31R-2, 132–135	1081.82			1.0	6.72	27.7		
31R-3, 10–15	1082.05			0.7	2.48	23.5		
31R-3, 45–50	1082.40	Cenomanian–Turonian	2	1.8	7.92	29.4	-23.82	-2.2
31R-3, 51–52	1082.46			0.0	7.18	33.1		
31R-3, 98–103	1082.93			1.6	2.11	28.7	-23.96	-0.65
31R-3, 127–129	1083.22			0.0	0.15	7.2		
31R-4, 0–1	1083.39			0.0	0.04	1.7		
31R-4, 13–18	1083.52			1.7	5.90	27.2	-26.06	-2.7
31R-4, 36–41	1083.75			0.3	0.41	15.7		
31R-4, 48–49	1083.87			1.9	5.43	26.5		
31R-4, 54–55	1083.93			2.0	0.18	6.7		
31R-4, 64–69	1084.03			1.8	6.06	32.1	-26.54	-2.13
31R-4, 109–111	1084.48			0.7	0.26	15.6		
31R-5, 97–98	1085.86			32.5	0.00			
31R-6, 32–33	1086.25			14.6	0.98	39.6	-19.57	1.2
32R-1, 0–1	1088.60			54.8	0.52	23.5		
32R-1, 30–31	1088.90			38.7	0.17	8.0		
32R-2, 83–84	1090.93			65.9	1.00	24.8		
32R-2, 144–146	1091.54			0.0	4.65	26.9		
32R-3, 48–49	1092.08			51.7	0.40	20.0		
32R-4, 0–1	1092.97			2.2	0.00			
32R-4, 26–28	1093.23			4.4	0.59	15.7		
32R-4, 57–58	1093.54			50.1	0.26	1.5		
32R-5, 23–27	1094.65			69.7	1.24	27.3		
32R-5, 45–46	1094.87			11.9	3.09	35.7		
32R-6, 70–72	1096.62			16.3	1.69	27.8	-26.76	-0.99
32R-7, 30–31	1097.72			0.0	0.66	23.4		
32R-7, 49–50	1097.91			1.9	0.26	7.2		
33R-1, 0–1	1098.20			4.9	0.43	9.6		
33R-1, 16–17	1098.36			2.6	0.24	9.0		
33R-1, 125–130	1099.45	Cenomanian		9.1	0.24	9.0		
33R-2, 138–139	1101.08			34.1	0.39	16.0		
33R-3, 13–15	1101.33			1.0	0.98	38.5		
33R-3, 91–95	1102.11			70.8	1.32	25.0		
33R-3, 139–140	1102.59			29.3	0.43	16.1		
33R-4, 0–1	1102.70			30.5	0.70	17.9		
33R-4, 19–20	1102.89			28.9	0.33	15.1		
33R-4, 133–137	1104.03			12.9	0.75	35.2		
33R-5, 11–13	1104.31			4.0	1.00	24.1	-25.95	1.1
33R-6, 13–14	1105.83			55.0	0.39	18.0		
33R-7, 14–15	1107.34			43.6	0.31	12.9		
34R-1, 126–127	1109.06		MCE	36.1	0.09	10.5		
34R-2, 10–11	1109.27			1.8	0.25	11.2		
34R-2, 94–98	1110.11			1.3	0.00			
34R-2, 100–102	1110.17			26.8	3.27	25.2	-27.25	-3.17
34R-2, 102–106	1110.19			67.3	1.33	19.5		
34R-3, 112–113	1111.79			19.9	0.56	27.5		
34R-4, 0–1	1112.13			48.2	0.44	19.1		

Table T1 (continued).

Core, section, interval (cm)	Depth (mbsf)	Age	OAE	CaCO ₃ (wt%)	TOC (wt%)	C _{org} /N _{tot} (atomic)	¹³ C (‰)	¹⁵ N (‰)
34R-4, 43–44	1112.56			17.6	0.21	7.5		
34R-4, 64–66	1112.77	Cenomanian		12.7	0.76	85.3		
34R-5, 36–37	1113.40			49.6	0.11	7.6		
43R-1, 46–49	1193.96			3.2	0.56	13.5		
43R-2, 34–36	1195.37			27.2	0.82	21.9	-25.13	1.4
43R-2, 88–92	1195.91			46.6	2.20	23.1	-27.13	-1.98
43R-3, 0–1	1196.55			1.9	0.52	11.6		
43R-3, 31–32	1196.86		1d	25.9	0.07	4.1	-25.56	2.6
43R-4, 146–147	1199.41			47.5	1.27	23.3		
43R-5, 104–106	1200.51			14.0	1.77	29.8	-25.13	1.4
43R-6, 0–1	1201.00			9.2	0.33	8.6		
43R-6, 57–59	1201.57	Albian–Cenomanian		10.4	0.60	12.9		
44R-1, 0–1	1203.20			51.8	1.36	23.8		
44R-1, 33–35	1203.53			3.2	0.59	13.5		
44R-2, 123–125	1205.96			16.0	0.09	6.1		
44R-3, 0–1	1206.20			11.2	0.00			
44R-3, 71–72	1206.91			36.1	0.60	19.2		
44R-4, 60–62	1208.34			1.3	0.38	11.4		
44R-5, 69–71	1209.97			19.9	0.62	17.3		
44R-7, 61–63	1212.97			37.4	2.12	18.9	-28.28	-2.45
55R-1, 70–71	1309.90			13.4	0.78	26.1	-25.265	1.40
55R-2, 0–1	1310.70			49.0	1.80	18.0	-26.8	-2
55R-3, 39–40	1312.59			42.5	0.54	14.8		
55R-4, 50–51	1314.20		1c	30.2	0.86	21.1	-25.21	1.30
58R-1, 66–68	1338.76			21.1	1.15	21.3		
58R-2, 60–62	1340.20			2.9	1.18	26.9		
58R-3, 57–59	1341.67			2.0	0.76	18.3		
58R-4, 56–58	1342.66			2.1	0.90	16.0		
59R-1, 90–92	1345.00			2.7	0.62	12.9		
60R-5, 76–78	1360.36			2.2	0.70	13.6		
61R-2, 63–65	1365.33			8.7	1.02	22.4		
62R-6, 118–120	1381.58			1.7	0.77	15.0		
63R-3, 69–71	1386.19			0.0	0.79	19.7		
63R-4, 70–72	1387.70			0.0	0.78	20.1		
65R-6, 40–42	1409.70			0.0	0.89	16.2		
66R-1, 93–96	1412.23			0.8	0.81	11.7		
67R-1, 80–82	1421.70			0.0	0.82	15.4		
68R-6, 76–78	1438.76			0.0	0.78	14.4		
69R-3, 45–47	1443.25			0.0	0.79	14.0		
71R-4, 118–120	1464.88			0.0	4.09	21.3	-27.275	-1.8
72R-2, 72–74	1471.12			1.5	0.73	12.9		
72R-5, 112–114	1475.85			14.5	2.06	32.2		
73R-1, 111–112	1479.61			1.3	2.78	29.7	-24.01	1.6
73R-2, 13–14	1480.13			1.1	0.87	14.6		
73R-3, 0–1	1481.50	Albian		1.1	2.09	20.9		
73R-3, 46–47	1481.96			1.1	2.63	21.5	-26.86	-1.18
73R-3, 60–62	1482.10			1.5	1.70	19.5		
73R-4, 31–32	1483.31		?	1.1	3.20	21.5	-26.38	-1.22
73R-5, 69–70	1485.19			1.6	1.25	18.7		
73R-6, 0–1	1486.00			0.2	0.72	15.9		
73R-6, 49–50	1486.49			1.6	0.84	15.1		
74R-3, 32–34	1491.42			1.1	2.10	21.6	-25.75	-0.79
74R-4, 33–35	1492.93			20.2	0.67	91.7		
75R-4, 76–79	1502.96			1.5	1.34	18.3		
76R-1, 119–122	1508.49			5.2	1.07	16.4		
77R-3, 109–111	1520.99			8.8	0.96	15.6		
78R-1, 133–135	1527.83			3.0	1.31	15.1		
79R-1, 62–64	1536.82			13.7	0.99	15.6		
79R-4, 54–56	1541.24			5.9	1.05	16.1	-24.18	-1.35
79R-5, 108–110	1543.28			0.0	0.74	16.7		
79R-5, 123–125	1543.43			8.8	0.99	17.9	-24.29	1.8
79R-5, 145–148	1543.65			15.0	0.85	18.1		
79R-6, 46–48	1544.16			0.0	3.76	23.5	-26.99	-0.95
80R-1, 5–7	1545.85			10.6	0.56	11.1		
80R-2, 120–122	1548.50			9.3	1.12	49.8		
80R-3, 129–131	1550.09			0.6	0.70	14.8		
81R-1, 81–83	1556.21			0.0	1.29	20.1		
81R-6, 45–47	1562.57			6.0	1.27	17.6		
82R-1, 0–1	1565.00			23.5	0.50	30.5		

Table T1 (continued).

Core, section, interval (cm)	Depth (mbsf)	Age	OAE	CaCO ₃ (wt%)	TOC (wt%)	C _{org} /N _{tot} (atomic)	¹³ C (‰)	¹⁵ N (‰)
82R-1, 6–9	1565.06			3.5	0.22	5.1		
83R-1, 103–105	1575.53			6.3	1.08	20.2		
84R-2, 79–81	1586.49			5.5	1.11	15.7		
85R-1, 128–130	1588.98			7.5	1.12	15.3		
86R-5, 8–10	1600.88			4.7	1.34	20.1		
87R-4, 118–121	1610.22			6.7	1.28	17.3		
91R-1, 114–116	1643.94			3.2	1.24	17.7		
92R-6, 27–30	1660.27			2.1	1.39	23.6		
93R-2, 58–60	1664.18			4.3	1.57	21.2		
94R-1, 8–9	1671.88			6.1	1.89	27.3		
94R-2, 14–15	1673.40			25.9	0.29	17.2	-24.37	1.0
94R-3, 47–48	1675.12			25.4	0.26	14.8		
94R-3, 102–104	1675.67	Albian		2.4	1.96	29.0	-23.81	-1.84
94R-4, 0–1	1676.15			7.0	1.58	20.5	-23.59	
94R-4, 31–32	1676.46			13.8	7.41	39.4	-21.85	-2
94R-4, 32–33	1676.47			1.2	4.27	35.6	-23.08	-1.08
94R-4, 142–144	1677.57			17.1	7.80	38.2	-22.18	-1.4
94R-5, 36–37	1677.95			27.1	6.32	41.1		
94R-5, 37–39	1677.96			9.4	7.74	33.3	-23.69	-2.09
94R-5, 71–72	1678.30			3.8	1.84	30.8		
94R-5, 89–91	1678.48			3.7	4.80	29.9	-23.14	-0.62
94R-6, 0–1	1679.09			8.7	1.51	22.1		
94R-6, 12–14	1679.21			7.0	1.82	20.0	-23.47	1.0
94R-6, 34–35	1679.43			10.1	1.74	24.7		
94R-CC, 23–24	1680.13			8.2	1.45	21.1	-23.75	1.3
96R-2, 58–61	1692.91	Aptian–Albian		4.0	1.32	16.0		
97R-2, 1–3	1702.01			0.9	0.36	9.2	-24.52	2.36
97R-2, 75–77	1702.75			7.6	1.09	14.2		
97R-5, 55–57	1706.43			4.0	1.68	24.5		

Notes: Age determinations from Shipboard Scientific Party (2004) and S. Gardin (pers. comm.). OAE = oceanic anoxic event, MCE = mid-Cenomanian event, ? = undetermined.

Table T2. Rock-eval pyrolysis results for selected samples, Site 1276.

Core, section, interval (cm)	Depth (mbfs)	Age	OAE	TOC (wt%)	T_{\max} (°C)	S_1 (mg HC/g)	S_2 (mg HC/g)	S_3 (mg CO ₂ /g)	PI	S_2/S_3	PC (%)	HI	OI
210-1276A-													
30R-4, 47–48	1074.10			6.65	419	0.11	16.65	1.31	0.01	12.7	1.4	270	21
30R-4, 115–116	1074.78	Turonian		1.38	429	0.03	0.67	0.44	0.05	1.5	0.1	52	34
30R-5, 33–34	1075.46			1.14	427	0.02	0.79	0.21	0.03	3.8	0.1	67	18
31R-1, 140–142	1080.40			6.54	420	0.09	16.77	0.56	0.01	29.9	1.4	271	9
31R-2, 59–62	1081.09			11.67	409	0.41	47.21	3.97	0.01	11.9	4.3	417	35
31R-2, 132–135	1081.82			6.72	409	0.17	19.74	1.72	0.01	11.5	1.7	320	28
31R-3, 45–50	1082.40	Cenomanian–Turonian	2	7.92	406	0.22	29.28	2.08	0.01	14.1	2.5	379	27
31R-3, 98–103	1082.93			2.11	423	0.03	2.22	0.9	0.01	2.5	0.2	120	48
31R-4, 13–18	1083.52			5.90	411	0.12	21.62	1.77	0.01	12.2	1.9	333	27
31R-4, 64–69	1084.03			6.06	413	0.12	15.48	1.53	0.01	10.1	1.4	281	28
32R-2, 144–146	1091.54			4.65	422	0.06	7.8	1.4	0.01	5.6	0.7	167	30
32R-5, 45–46	1094.87			3.09	429	0.04	2.94	1.43	0.01	2.1	0.3	87	42
32R-6, 70–72	1096.62			1.69	424	0.02	1.12	1.21	0.01	0.9	0.1	61	66
33R-1, 125–130	1099.45			0.24	421	0.01	0.3	0.71	0.03	0.4	0.0	34	82
33R-3, 13–15	1101.33			0.98	413	0.01	0.13	0.33	0.07	0.4	0.0	14	35
33R-3, 91–95	1102.11	Cenomanian		1.32	423	0.02	3.06	1.2	0.01	2.6	0.3	180	71
33R-5, 11–13	1104.31			1.00	412	0.01	0.12	0.33	0.08	0.4	0.0	12	34
34R-2, 100–102	1110.17	MCE		3.27	422	0.04	4.98	1.9	0.01	2.6	0.4	146	56
34R-2, 102–106	1110.19			1.33	426	0.02	2.74	1.31	0.01	2.1	0.3	149	71
34R-4, 64–66	1112.77			0.76	425	0.01	0.08	0.8	0.08	0.1	0.0	10	104
43R-2, 88–92	1195.91			2.20	422	0.04	4.50	1.28	0.01	3.5	0.4	186	53
43R-3, 31–32	1196.86			0.07		0.00	0.02	0.42	0.13	0.0	0.0	11	221
43R-5, 104–106	1200.51	Albian–Cenomanian	1d	1.77	427	0.00	0.25	0.66	0.01	0.4	0.0	15	40
44R-3, 0–1	1206.20			0.09	429	0.01	0.03	0.30	0.14	0.1	0.0	18	176
44R-7, 61–63	1212.97			0.62	424	0.04	4.13	1.25	0.01	3.3	0.4	160	48
55R-1, 70–71	1309.90			0.78	426	0.01	0.22	0.42	0.05	0.5	0.0	26	50
55R-2, 0–1	1310.70		1c	1.80	425	0.02	2.68	1.41	0.01	1.9	0.3	131	69
55R-4, 50–51	1314.20			0.86	420	0.01	0.22	0.59	0.05	0.4	0.0	31	83
71R-4, 118–120	1464.88			4.09	423	0.05	7.54	0.73	0.01	10.3	0.7	201	19
72R-5, 112–114	1475.85			2.06	429	0.02	2.43	0.93	0.01	2.6	0.3	90	34
73R-1, 111–112	1479.61			2.78	430	0.02	0.87	0.43	0.02	2.0	0.1	34	16
73R-3, 46–47	1481.96			2.63	424	0.04	5.07	0.52	0.01	9.8	0.4	177	18
73R-4, 31–32	1483.31	?		3.20	425	0.05	5.59	0.57	0.01	9.8	0.5	201	21
73R-6, 49–50	1486.49			0.84	424	0.01	0.43	0.21	0.02	2.0	0.0	40	19
74R-3, 32–34	1491.42			2.10	427	0.02	1.65	0.2	0.01	8.3	0.1	91	11
79R-4, 54–56	1541.24	Albian		1.05	426	0.01	0.22	0.33	0.03	0.7	0.0	22	33
79R-5, 123–125	1543.43			0.99	428	0.01	0.23	0.26	0.02	0.9	0.0	25	28
79R-6, 46–48	1544.16			3.76	425	0.06	7.17	0.64	0.01	11.2	0.6	212	19
94R-1, 8–9	1671.88			1.89	431	0.03	0.65	0.39	0.04	1.7	0.1	32	19
94R-3, 102–104	1675.67			1.96	432	0.03	0.64	0.34	0.04	1.9	0.1	34	18
94R-4, 32–33	1676.47		1b	4.27	413	0.24	12.58	0.4	0.02	31.5	1.1	316	10
94R-4, 142–144	1677.57			7.80	408	1.03	36.92	1.39	0.03	26.6	3.2	462	17
94R-5, 37–39	1677.96			7.74	411	0.78	29.42	1.24	0.03	23.7	2.6	406	17
94R-5, 89–91	1678.48			4.80	414	0.24	14.58	0.45	0.02	32.4	1.3	331	10
94R-6, 12–14	1679.21			1.82	429	0.03	0.66	0.48	0.04	1.4	0.1	40	29
94R-CC, 23–24	1680.13			1.45	431	0.02	0.48	0.53	0.03	0.9	0.1	29	32

Notes: Age determinations from Shipboard Scientific Party (2004) and S. Gardin (pers. comm.). OAE = oceanic anoxic event, MCE = mid-Cenomanian event, ? = undetermined. TOC = total organic carbon, S_1 = free hydrocarbon (gas and oil), S_2 = hydrocarbon generated through thermal cracking of nonvolatile organic matter, S_3 = CO₂ produced during pyrolysis of kerogen, HC = hydrocarbon, PI = productivity index, PC = pyrolyzed carbon, HI = hydrogen index, OI = oxygen index.

Table T3. Trace elements and element oxide abundances for selected samples, Site 1276.

Core, section, interval (cm)	Depth (mbsf)	Age	TOC (wt%)	Element oxides (wt%)					Trace elements (µg/g)									
				Al ₂ O ₃	TiO ₂	Fe ₂ O ₃	MgO	K ₂ O	Ba	Cd	Cr	Cu	Mo	Re	U	V	Zn	
210-1276A-																		
30R-4, 47–48	1074.10	Turonian	6.65	6.38	0.43	3.17	0.94	2.22	1402	3.77	234	370	0.083	6.7	463	433		
30R-5, 33–34	1075.46		1.14	6.04	0.42	2.86	0.98	2.03	593	1.27	105	36	0.014	3.3	103	130		
31R-2, 59–62	1081.09		11.67	3.83	0.23	5.34	0.62	1.48	245	1.83	124	75	22	0.110	4.1	213	127	
31R-3, 45–50	1082.40	Cenomanian–Turonian	2	7.92	5.69	0.34	4.19	0.83	1.47	272	2.01	126	87	5	0.056	7.4	137	39
31R-3, 98–103	1082.93		2.11	5.46	0.37	5.55	1.00	1.87	308	1.74	157	72		0.055	1.9	116	83	
31R-4, 13–18	1083.52		5.90	6.53	0.39	4.71	0.91	2.05	330	1.89	123	77		0.165	4.4	133	216	
32R-6, 70–72	1096.62		1.69	5.37	0.32	2.96	0.92	1.84	431	1.88	136	101		0.059	2.5	221	200	
33R-5, 11–13	1104.31	Cenomanian	1.00	5.96	0.36	2.99	1.09	1.99	363	1.93	97	101			1.6	92	121	
34R-2, 100–102	1110.17		3.27	5.30	0.28	3.60	0.85	1.65	280	2.43	124	89	7	0.125	3.5	447	242	
43R-2, 88–92	1195.91		2.20	3.77	0.18	3.07	0.53	1.08	803	0.34	79	41	6	0.043	3.2	184	160	
43R-3, 31–32	1196.86	Albian–Cenomanian	1d	0.07	5.09	0.24	2.83	0.76	1.70	362		80	21		0.7	50	58	
43R-5, 104–106	1200.51		1.77	6.86	0.41	2.96	0.91	2.07	522	0.45	108	33			1.7	79	93	
44R-7, 61–63	1212.97		0.62	4.57	0.17	3.41	0.48	0.98	860	1.58	111	50	9	0.052	3.2	277	338	
55R-1, 70–73	1309.90		0.78	3.67	0.32	1.94	0.57	1.57	344	1.79	69	14			1.9	50	99	
55R-2, 0–1	1310.70		1c	1.80	3.80	0.16	3.26	0.59	1.27	194	0.24	103	34	5	0.013	0.9	103	89
55R-4, 50–52	1314.20		0.86	5.72	0.27	2.75	0.92	1.91	291		99	43			1.5	76	139	
71R-4, 118–120	1464.88		4.09	6.36	0.35	5.10	1.09	2.41	440	1.32	211	82		0.016	2.6	138	197	
73R-1, 111–112	1479.61		2.78	8.63	0.37	3.86	1.21	3.00	523	1.22	150	58			1.6	103	180	
73R-3, 46–47	1481.96		?	2.63	6.84	0.37	5.07	1.13	2.49	457	1.19	181	107	5	0.014	2.5	148	215
73R-4, 31–32	1483.31		3.20	7.47	0.35	5.20	1.15	2.65	453	1.73	192	84		0.015	2.3	150	165	
74R-3, 32–34	1491.42	Albian		2.10	7.81	0.37	4.26	1.18	2.84	449	1.67	142	64		2.1	107	240	
79R-4, 54–56	1541.24		1.05	9.02	0.49	5.21	1.24	2.57	428	1.56	149	39			2.0	107	121	
79R-6, 46–48	1544.16		3.76	6.08	0.42	4.33	1.02	2.60	407	1.69	209	89		0.015	2.8	143	198	
94R-3, 102–104	1675.67		1.96	8.97	0.45	4.41	1.03	2.99	387	1.20	147	50			2.0	112	104	
94R-4, 32–33	1676.47		4.27	9.33	0.44	4.64	0.62	2.02	360	2.12	176	79	70	0.100	4.6	112	162	
94R-4, 142–144	1677.57		7.80	6.79	0.33	6.44	0.85	2.54	293	3.35	130	80	181	0.217	8.7	141	480	
94R-5, 37–39	1677.96		7.74	7.01	0.35	4.93	0.70	2.15	293	2.12	132	69	111	0.306	9.7	143	192	
94R-5, 89–91	1678.48		4.80	7.59	0.41	6.78	0.85	2.43	335	7.51	201	82	34	0.182	3.4	331	548	
94R-CC, 23–24	1680.13		1.45	9.04	0.47	4.48	1.03	2.77	362	1.20	144	37			2.0		105	

Notes: Age determinations are from Shipboard Scientific Party (2004) and S. Gardin (pers. comm.). OAE = oceanic anoxic event, MCE = mid-Cenomanian event, ? = undetermined. TOC = total organic carbon.

Table T4. Element/Al ratios for selected samples, Site 1276.

Core, section, interval (cm)	Depth (mbsf)	Age	OAE	TOC (wt%)	Major elements					Minor elements (10^{-4})								
					Ti/Al	Fe/Al	Mg/Al	K/Al	Ba/Al	Cd/Al	Cr/Al	Cu/Al	Mo/Al	Re/Al	U/Al	V/Al	Zn/Al	Cd/Al
210-1276A-																		
30R-4, 47–48	1074.10	Turonian		6.65	0.067	0.50	0.15	0.35	220	0.59	36.6	58		0.013	1.05	73	68	0.59
30R-5, 33–34	1075.46			1.14	0.070	0.47	0.16	0.34	98	0.21	17.4	6		0.002	0.55	17	22	0.21
31R-2, 59–62	1081.09			11.67	0.059	1.39	0.16	0.39	64	0.48	32.4	20	6	0.029	1.07	56	33	0.48
31R-3, 45–50	1082.40	Cenomanian–Turonian	2	7.92	0.059	0.74	0.15	0.26	48	0.35	22.1	15	1	0.010	1.30	24	7	0.35
31R-3, 98–103	1082.93			2.11	0.069	1.02	0.18	0.34	56	0.32	28.7	13		0.010	0.34	21	15	0.32
31R-4, 13–18	1083.52			5.90	0.060	0.72	0.14	0.31	50	0.29	18.9	12		0.025	0.67	20	33	0.29
32R-6, 70–72	1096.62			1.69	0.060	0.55	0.17	0.34	80	0.35	25.4	19		0.011	0.47	41	37	0.35
33R-5, 11–13	1104.31	Cenomanian	MCE	1.00	0.061	0.50	0.18	0.33	61	0.32	16.3	17		0.26	15	20	0.32	
34R-2, 100–102	1110.17			3.27	0.052	0.68	0.16	0.31	53	0.46	23.5	17	1	0.024	0.66	84	46	0.46
43R-2, 88–92	1119.91			2.20	0.048	0.81	0.14	0.29	213	0.09	20.8	11	2	0.011	0.84	49	42	0.09
43R-3, 31–32	1119.86	Albian–Cenomanian	1d	0.07	0.047	0.56	0.15	0.33	71		15.7	4		0.14	10	11		
43R-5, 104–106	1200.51			1.77	0.060	0.43	0.13	0.30	76	0.07	15.8	5		0.24	12	14	0.07	
44R-7, 61–63	1212.97			0.62	0.038	0.75	0.11	0.21	188	0.35	24.3	11	2	0.011	0.70	60	74	0.35
55R-1, 70–73	1309.90			0.78	0.088	0.53	0.16	0.43	94	0.49	18.8	4		0.51	14	27	0.49	
55R-2, 0–1	1310.70		1c	1.80	0.042	0.86	0.16	0.33	51	0.06	27.2	9	1	0.003	0.24	27	24	0.06
55R-4, 50–52	1314.20			0.86	0.047	0.48	0.16	0.33	51		17.3	8		0.26	13	24		
71R-4, 118–120	1464.88			4.09	0.055	0.80	0.17	0.38	69	0.21	33.1	13		0.003	0.41	22	31	0.21
73R-1, 111–112	1479.61	Albian		2.78	0.043	0.45	0.14	0.35	61	0.14	17.3	7		0.19	12	21	0.14	
73R-3, 46–47	1481.96		?	2.63	0.054	0.74	0.17	0.36	67	0.17	26.5	16	1	0.002	0.37	22	31	0.17
73R-4, 31–32	1483.31			3.20	0.047	0.70	0.15	0.35	61	0.23	25.7	11		0.002	0.30	20	22	0.23
74R-3, 32–34	1491.42			2.10	0.048	0.55	0.15	0.36	57	0.21	18.2	8		0.27	14	31	0.21	
79R-4, 54–56	1541.24			1.05	0.054	0.58	0.14	0.29	48	0.17	16.5	4		0.22	12	13	0.17	
79R-6, 46–48	1544.16			3.76	0.069	0.71	0.17	0.43	67	0.28	34.3	15		0.003	0.47	23	32	0.28
94R-3, 102–104	1675.67			1.96	0.050	0.49	0.12	0.33	43	0.13	16.3	6		0.22	12	12	0.13	
94R-4, 32–33	1676.47			4.27	0.047	0.50	0.07	0.22	39	0.23	18.9	9	7	0.011	0.49	12	17	0.23
94R-4, 142–144	1677.57	Aptian–Albian	1b	7.80	0.049	0.95	0.13	0.37	43	0.49	19.1	12	27	0.032	1.28	21	71	0.49
94R-5, 37–39	1677.96			7.74	0.050	0.70	0.10	0.31	42	0.30	18.9	10	16	0.044	1.38	20	27	0.30
94R-5, 89–91	1678.48			4.80	0.054	0.89	0.11	0.32	44	0.99	26.5	11	4	0.024	0.45	44	72	0.99
94R-CC, 23–24	1680.13			1.45	0.052	0.50	0.11	0.31	40	0.13	15.9	4		0.22	11	12	0.13	

Notes: Age determinations are from Shipboard Scientific Party (2004) and S. Gardin (pers. comm.). OAE = oceanic anoxic event, MCE = mid-Cenomanian event, ? = undetermined. TOC = total organic carbon.